

## Tunable Broadband Mid-IR OPO/DFG System for Near-field Imaging and Spectroscopy

---

**Abstract:** We combine a mid-IR OPO/DFG system from APE GmbH with a scanning probe system from Anasys Inst. to demonstrate a state-of-the-art tool for nanospectroscopy. The light source has a FWHM bandwidth of  $150\text{ cm}^{-1}$  -  $200\text{ cm}^{-1}$  and a tuning range of  $666 - 2222\text{ cm}^{-1}$  ( $4.5 - 15\text{ }\mu\text{m}$ ) with up to 20 mW output power, enabling direct sub-ensemble vibrational spectroscopy of material systems with nanometer-scale chemical or structural heterogeneity. We demonstrate near-field imaging and spectroscopy on a range of condensed matter materials, showing measurements sensitive to nanoscale chemical composition, film thickness, and local molecular ordering, all with cutting-edge signal quality. The measurement capabilities of this combined system promise new insight in the understanding and engineering of advanced materials.

**Authors:** Markus B. Raschke, University of Colorado, Boulder & Ingo Rimke, Director of R&D, APE GmbH

---

### Introduction

The properties of chemically or structurally heterogeneous materials are often determined by intermolecular interactions over nanometer length scales. Measurement tools that can access these length scales with chemical specificity are thus highly desirable in understanding and engineering many advanced materials. Broadband infrared scattering scanning near-field optical microscopy (IR *s*-SNOM) is one such technique which can perform chemical nanoimaging and nanospectroscopy with the desired spatial resolution and chemical specificity [1]. Based on the scattering response of a sample coupled in the near-field to the plasmonic enhancement of a metalized scanning probe tip, IR *s*-SNOM is broadly compatible with a variety of light sources and detection modalities [2]. Here we describe the combination of a mid-IR OPO/DFG system from APE GmbH with a state-of-the-art *s*-SNOM system from Anasys Inst., characterize its performance, and demonstrate its use on several representative sample systems.

### Description of the OPO/DFG Source

The source described here is a two-step nonlinear mixing system consisting of a synchronously pumped Optical Parametric Oscillator (OPO) and a Difference Frequency Generation (DFG) stage, designed by APE GmbH. It is pumped by an ultrafast modelocked near-IR laser (FLINT, Light Conversion). The pump laser, based on a Yb:KGW crystal, generates 7 W of average power at 1032 nm. The pulses are  $<90$  fs long and occur at 76 MHz. The pump beam drives an optical parametric oscillator (OPO, Levante IR, APE GmbH) based on a fanned periodically polled lithium niobate (PPLN) crystal. The OPO generates signal pulses between  $1.3\text{-}2.0\text{ }\mu\text{m}$  ( $5000 - 7700\text{ cm}^{-1}$ ) and idler pulses between  $2.2\text{-}4.8\text{ }\mu\text{m}$  ( $2080 - 4550\text{ cm}^{-1}$ ), tuned automatically by adjusting the cavity length via a piezo-mounted end mirror and lineally translating the crystal via a motorized actuator. The signal beam has an average power of  $\sim 1.5$  W, while the idler beam has an average power of  $\sim 0.6$  W. A spectrum of the signal is continuously acquired and used in a computerized feedback loop for stability and automated tuning.

The signal and idler beams of the OPO are subsequently mixed in a critically phase matched nonlinear crystal for difference frequency generation of light between 666 - 2222  $\text{cm}^{-1}$  (4.5 - 15  $\mu\text{m}$ ) and further into the long wavelength range. The temporal and spatial overlap, and the phase matching angle, are adjusted using manual actuators.

### Characterization of OPO-DFG output

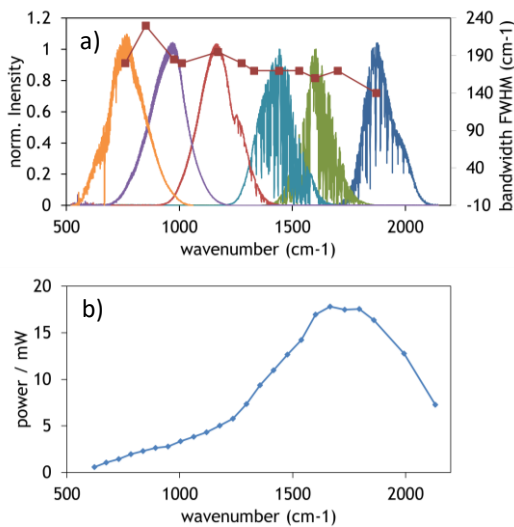


Figure 1: (a) normalized spectra of DFG output across the tunable range of the OPO-DFG system, their bandwidths (FWHM), and b) corresponding average powers.

The average power and spectral output of the DFG across its tunable range is shown in Fig. 1a. Mid-IR spectra were measured with a Thermo Nicolet 6700 FTIR spectrometer showing a bandwidth of 150 - 200  $\text{cm}^{-1}$  (FWHM). The spectral range covered by the DFG output encompasses a significant part of the “fingerprint region” for molecular spectra. This is giving access to key bending, stretching, and breathing modes commonly used for chemical identification. It can serve as probes of molecular disorder, structural orientation, and polymorphism, among other properties [1]. The output power of up to 20 mW and a useable spectral bandwidth of  $>300 \text{ cm}^{-1}$  (10dB level) outperforms other table top light sources by far.

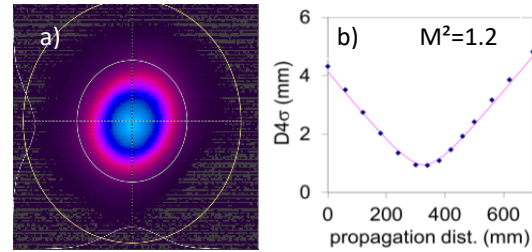


Figure 2: beam characteristics measured at 7.6  $\mu\text{m}$  (1315  $\text{cm}^{-1}$ )

a) beam profile and b) beam diameter measurements of  $D4\sigma$  in the horizontal direction as a function of propagation distance from an IR lens (blue circles). Fit (line) yields an  $M^2$  value of 1.2, showing a perfect Gaussian beam shape

Fig. 2a shows the spatial mode profile of the DFG output. It was measured with an IR beam camera (Spiricon Pyrocam IIIHR). The beam shape does show a perfect Gaussian beam profile with  $M^2$  of 1.2 as shown in Fig. 2b. A Gaussian beam shape with good focusing properties is ideal for IR *s*-SNOM to achieve a tight focus spot at the scanning probe tip, increasing the incident field intensity and thus the scattered signal.

### Demonstration measurements with *s*-SNOM

A schematic layout of the OPO/DFG source integrated in a standard IR *s*-SNOM setup is shown in Fig. 3a. The DFG output is incident on the 50-50 beamsplitter of an asymmetric Michelson interferometer. One arm is focused onto the apex of a scanning probe tip with a 90-degree off-axis parabolic mirror. Light from near-field tip-sample scattering travels back along this sample arm, reflects off the beamsplitter, and interferometrically combines at a Mercury Cadmium Telluride (MCT) detector with light retro-reflected from a movable reference arm. The tip is dithered at hundreds of kHz, and the portion of the detector’s output arising from near-field scattering at the tip apex is demodulated using a lock-in amplifier (not shown) at higher harmonics of the tip tapping frequency. Lock-in detection is essential for isolating the small tip-sample signal from much larger signals due to scattering from the tip or sample on their own.

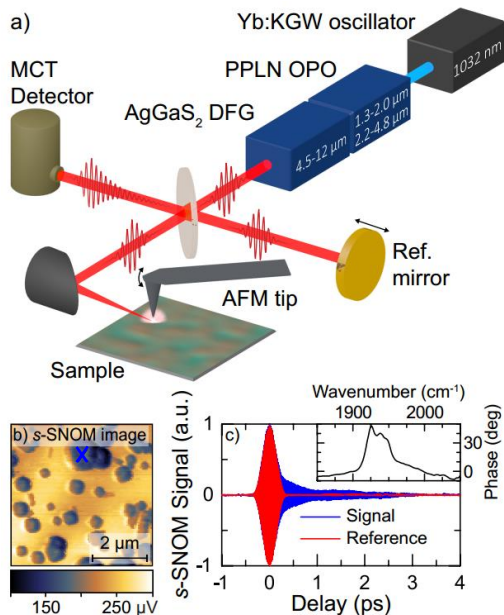


Figure 3: (a) Schematic layout of combined OPO/DFG and s-SNOM setup. (b) Example of broadband s-SNOM imaging, showing aggregates of RuOEP molecules. (c) Example of nano-spectroscopy, showing free-induction decay interferogram acquired at the location marked in (b) with the blue X. Reference from a separate Au sample. Corresponding phase spectrum (inset) shows resonant peaks of split RuOEP metal carbonyl mode.

Scanning the tip across a nanoscale region of a sample produces a map of nano-optical response, as shown in Fig. 3b. This image shows semi-crystalline aggregates of 2,3,7,8,12,13,17,18-octaethyl-21H,23H-porphine ruthenium(II)carbonyl (RuOEP) on a flat gold substrate. RuOEP is known to form 1D polymer-like arrangements over several stages of intermolecular ordering [3]. The DFG output was tuned to the blue end of its range, with a center wavenumber of 1940  $\text{cm}^{-1}$  and a full-width half-max bandwidth of  $\sim 150 \text{ cm}^{-1}$ . The image shows contrast in the broadband integrated optical response across the sample, arising from the relatively lower polarizability typical of molecular materials compared to metallic substrates.

By changing the relative path difference between sample and reference arms, one can further probe specific locations on the sample via nano-FTIR. Fig. 3c shows interferograms

produced by scanning the reference arm across the zero-delay position. A reference measurement on a non-resonant sample (shown in red) is required to normalize out inherent variations in laser power, tip scattering, mirror reflectivity, detector sensitivity, and other effects across the spectral range of interest. The reference interferogram is dominated by interference from the quasi-instantaneous response of metallic non-resonant scattering, essentially producing a linear autocorrelation of the laser pulse. In contrast, the interferogram from the sample location (shown in blue, location marked with a blue X in Fig. 3b) shows continuing interference at larger delays, known as free induction decay, arising from a longer-lived resonance in the probed sample region. Fourier transforming both signal and reference interferograms and normalizing one to the other results in a spectrum of the probed region under the tip apex (Fig. 3c inset). In this case, the resonant signature of the RuOEP metal carbonyl mode is clearly visible, split due to transition dipole coupling in crystalline domains, in which  $\pi$ -backbonding provides a sensitive probe of order and crystallinity [3].

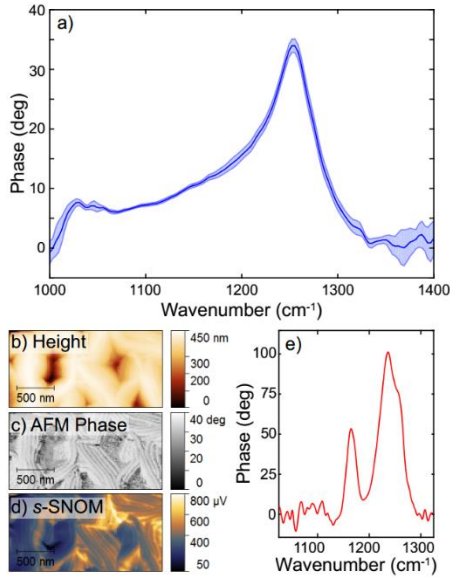


Figure 4: (a) Spectra from an SiO<sub>2</sub> surface showing an SiO<sub>2</sub> phonon mode, with error bars showing reproducibility over repeated measurements. (b-d) Broadband imaging of PTFE, showing local ordering. (e) Nanoscale spectrum of PTFE, showing the symmetric and asymmetric C-F stretching modes. SiO<sub>2</sub> data courtesy of E. A. Muller, PTFE data courtesy of B. Metzger. The sample was created by J. Allerbeck.

Fig. 4a shows a nano-FTIR spectrum, acquired in the same way as just described, of the phonon response of a thin film of SiO<sub>2</sub> 10s of nm thick, on crystalline Si [4]. The sample was provided by Anasys Inst. The blue shaded region shows the standard deviation of each wavenumber response from eight separate spectra acquired sequentially, as an indication of the signal-to-noise of the combined OPO/DFG IR *s*-SNOM setup. The darker blue line shows the average of these spectra. Each spectrum was acquired with a scan time of 100 s, using a lock-in time constant of 2 ms, and with a spectral resolution of 5 cm<sup>-1</sup>. The signal quality shown here is sufficient to not only resolve the phonon response, but to perform a more detailed analysis of peak position and line shape. Such factors depend sensitively on SiO<sub>2</sub> film thickness and doping levels, making such precision nanospectroscopy measurements highly desirable for mapping defects and optimizing nanoscale device performance [5].

Lastly, Fig. 4b-d show images of an aggregated film of polytetrafluoroethylene (PTFE, also known as Teflon™). Fig. 4b-c show height and AFM tapping phase images common to atomic force microscopy, acquired simultaneously with the IR *s*-SNOM map shown in Fig. 4d. PTFE polymers form ordered segments of high density and with significant variation in the degree of crystallinity, possibly with several crystalline phases [6]. A nanoscale spectrum from this sample is shown in Fig. 4e, with two peaks corresponding to the symmetric and antisymmetric C-F stretching mode of PTFE. Intermolecular coupling strongly affects the coherent dynamics and decay pathways of these modes, resulting in nanoscale variation in relative peak height, position, and linewidth [7]. The combination of spectral irradiance and bandwidth provided by this laser source allows for nanoscale spatial mapping of spectral variation across multiple resonances, such as these in PTFE, for powerful insight into sub-ensemble heterogeneity and intermolecular interactions.

## Conclusion

We present combination of a mid-IR OPO/DFG system from APE GmbH with an *s*-SNOM system from Anasys Inst. Pumped with a Yb:KGW modelocked laser, the PPLN-based OPO produces tunable signal and idler beams which are subsequently combined in a DFG crystal. The DFG output has a usable bandwidth of 300 cm<sup>-1</sup> (10dB level; 150 - 200 cm<sup>-1</sup> FWHM) and a tuning range of 666 - 2222 cm<sup>-1</sup> (4.5 - 15 μm) with up to 20 mW of output power, enabling spectroscopy of molecular vibrations in the fingerprint region with nanoscale spatial resolution. The system produces state-of-the-art IR *s*-SNOM spectra on a range of condensed matter sample systems, probing nanoscale chemical composition, film thickness and doping, and local molecular ordering. The capabilities of the combined setup enable measurements of chemical and structural heterogeneity, and associated intermolecular interactions, with nanometer spatial resolution,

promising new insight in the understanding and engineering of advanced materials.

## Update

APE is now offering the fully automated one-box laser source *Carmina* with the above described parameters. *Carmina* further includes a narrow-band mode for s-SNOM imaging as well as a narrow-band pulsed mode for photo-thermal AFM-IR applications.

## References

1. E. A. Muller, B. Pollard, M. B. Raschke, Infrared Chemical Nano-Imaging: Accessing Structure, Coupling, and Dynamics on Molecular Length Scales. *J. Phys. Chem. Lett.* **6**, 1275-1284 (2015).
2. J. M. Atkin, S. Berweger, A. C. Jones, M. B. Raschke, Nano-optical imaging and spectroscopy of order, phases, and domains in complex solids. *Adv. Phys.* **61**, 745-842 (2012).
3. A. A. Eigner, P. E. Konold, A. M. Massari, Infrared spectroscopic signatures of phase segregation in P3HT-porphyrin blends. *J. Phys. Chem. B.* **113**, 14549-54 (2009).
4. H. A. Bechtel, E. A. Muller, R. L. Olmon, M. C. Martin, M. B. Raschke, Ultrabroadband infrared nanospectroscopic imaging. *Proc. Natl. Acad. Sci. U.S.A.* **111**, 7191-7196 (2014).
5. L. M. Zhang *et al.*, Near-field spectroscopy of silicon dioxide thin films. *Phys. Rev. B.* **85**, 75419 (2012).
6. A. Serov *et al.*, Poly(tetrafluoroethylene) sputtering in a gas aggregation source for fabrication of nano-structured deposits. *Surf. Coatings Technol.* **254**, 319-326 (2014).
7. J. M. Atkin, P. M. Sass, P. E. Teichen, J. D. Eaves, M. B. Raschke, Nanoscale Probing of Dynamics in Local Molecular Environments. *J. Phys. Chem. Lett.* **6**, 4616-4621 (2015).